Adsorption 5, 145–158 (1999)
© 1999 Kluwer Academic Publishers. Manufactured in The Netherlands.

Pure and Binary Gas Adsorption Equilibria and Kinetics of Methane and Nitrogen on 4A Zeolite by Isotope Exchange Technique*

R.J. MOHR, D. VORKAPIC, M.B. RAO AND S. SIRCAR
Air Products and Chemicals, Inc., 7201 Hamilton Boulevard, Allentown, PA 18195-1501

Abstract. The Isotope Exchange Technique (IET) was used to simultaneously measure pure and binary gas adsorption equilibria and kinetics (self-diffusivities) of CH_4 and N_2 on pelletized 4A zeolite. The experiment was carried out isothermally without disturbing the adsorbed phase. CH_4 was selectively adsorbed over N_2 by the zeolite because of its higher polarizability. The multi-site Langmuir model described the pure gas and binary adsorption equilibria fairly well at three different temperatures. The selectivity of adsorption of CH_4 over N_2 increased with increasing pressure at constant gas phase composition and temperature. This curious behavior was caused by the differences in the sizes of the adsorbates. The diffusion of CH_4 and N_2 into the zeolite was an activated process and the Fickian diffusion model described the uptake of both pure gases and their mixtures. The self-diffusivity of N_2 was an order of magnitude larger than that for CH_4. The pure gas self-diffusivities for both components were constants over a large range of surface coverages ($0 < \theta < 0.5$). The self-diffusivities of CH_4 and N_2 from their binary mixtures were not affected by the presence of each other, compared to their pure gas self-diffusivities at identical surface coverages.

Keywords: kinetics, isotope-exchange, nitrogen, adsorption, methane, zeolite, equilibria

Introduction

The recently developed Isotope Exchange Technique (IET) can be used to simultaneously measure pure and multicomponent gas adsorption equilibria and kinetics in a single isothermal experiment without disturbing the overall adsorbed phase (Rynders et al., 1997). The key advantages of the technique are as follows:

(a) Complete control over the equilibrium state of the adsorption system during the experiment. It is defined by the chosen values of the system temperature (T), gas phase pressure (P) and mole fraction of component i (y_i).
(b) Absolutely isothermal ad(de)sorption process.
(c) Relative ease of experimental procedure.

The general principle of IET consists of equilibrating an adsorbent mass in a closed system with a pure gas i ($y_i = 1$) at a given P and T or with a multicomponent gas mixture of i components ($i \geq 2$) at P, T and y_i. The pure gas i or the ith component of the mixture may consist of a bulk isotope (mole fraction y_i^{*0}) and one or more trace isotopes (j varieties with mole fractions of y_{ij}^{*0}). The total mole fraction of component i is given by:

$$y_i^{*0} + \sum_j y_{ij}^{*0} = y_i \tag{1}$$

The gas phase mole fractions of the bulk and trace isotopes of component i are changed to y_i^{**} and y_{ij}^{**}, respectively, at the start of the IET experiment (time $t = 0$) while maintaining P, T and y_i constants:

$$y_i^{**} + \sum_j y_{ij}^{**} = y_i \tag{2}$$

The gas phase mole fractions of the bulk or trace isotopes of component i are then monitored as functions of time ($y_i^*(t)$ and $y_{ij}^*(t)$) until they reach a new isotopic

*© 1998, Air Products and Chemicals, Inc.

equilibrium state ($y_i^{*\infty}$ and $y_{ij}^{*\infty}$):

$$y_i^*(t) + \sum_j y_{ij}^{**}(t) = y_i^{*\infty} + \sum_j y_{ij}^{*\infty} = y_i \qquad (3)$$

A chemical potential driving force for transport of the isotope species of component i is created by the IET experiment. The isotopes of component i are transported from the gas phase to the adsorbed phase or removed from the adsorbed phase to the gas phase depending on whether $y_{ij}^{**} \gtrless y_{ij}^{*0}$. However, there is no net flux of the component i at any time $t(J_i(t))$ during the IET experiment because the system remains in equilibrium at P, T and y_i:

$$J_i(t) = J_i^*(t) + \sum_j J_{ij}^*(t) = 0 \qquad (4)$$

where $J_i^*(t)$ and $J_{ij}^*(t)$ are respectively, the fluxes of the bulk and trace isotopes of component i at time t during the IET experiment.

The Gibbsian Surface Excesses (GSE) are used to describe the extents of adsorption (n_i^{m}) of component i (pure gas or mixture) as well as those for the bulk ($n_i^{*\mathrm{m}}$) and trace ($n_{ij}^{*\mathrm{m}}$) isotopes of component i. The GSE for component i (n_i^{m}) remains constant during the IET experiment (constant P, T and y_i) but the variables ($n_i^{*\mathrm{m}}$) and ($n_{ij}^{*\mathrm{m}}$) change with time:

$$\begin{aligned} n_i^{*\mathrm{m}}(t) + \sum_j n_{ij}^{*\mathrm{m}}(t) &= n_i^{*\mathrm{m}}(0) + \sum_j n_{ij}^{*\mathrm{m}}(0) \\ &= n_i^{*\mathrm{m}}(\infty) + \sum_j n_{ij}^{*\mathrm{m}}(\infty) = n_i^{\mathrm{m}} \end{aligned} \qquad (5)$$

Where $n_i^{*\mathrm{m}}(t)$ and $n_{ij}^{*\mathrm{m}}(t)$ are, respectively the transient GSE for bulk and trace isotopes of component i at time t. The corresponding variables represented by (0) and (∞) are, respectively, the equilibrium GSE at the start ($t = 0$, y_i^{*0}, y_{ij}^{*0}) and at the end ($t = \infty$, $y_i^{*\infty}$, $y_{ij}^{*\infty}$) of the IET experiment.

The GSE is the true experimental variable for measuring the extent of adsorption (Gibbs, 1928; Sircar, 1985, 1996). It is generally defined by:

$$n_i^{\mathrm{m}} = n_i^{\mathrm{a}} - v^{\mathrm{a}}\rho y_i \qquad (6)$$

where n_i^{a} is the actual amount of component i adsorbed, v^{a} is the actual volume of the adsorbed phase, and ρ is the gas phase density. Equation (6) can be used to define both transient and equilibrium GSE for component i (pure gas or mixture) as well as its isotopes.

It can be shown that the equilibrium GSE for component i (n_i^{m}) at P, T and y_i is given by (Rynders et al., 1997):

$$\begin{aligned} &n_i^{\mathrm{m}}(P, T, y_i) \\ &\quad = (V\rho y_i)\left[\frac{y_{ij}^{**} - y_{ij}^{*\infty}}{y_{ij}^{**} - y_{ij}^{*0}}\right] \quad i, j = 1, 2 \ldots \end{aligned} \qquad (7)$$

where the variable V is the total specific helium volume of the closed adsorption system of the IET experiment. ρ is the gas phase density at P and T. Relationships analogous to Eq. (7) can also be derived using the bulk isotope mole fractions of component i.

It can also be shown that the transient fractional uptake (or loss) of the trace jth isotope of component i ($f_{ij}^*(t)$) and the rate of change of the corresponding GSE at constant P, T and y_i are given by (Rynders et al., 1997):

$$f_{ij}^*(t) = \left[\frac{n_{ij}^{*\mathrm{m}}(t) - n_{ij}^{*\mathrm{m}}(0)}{n_{ij}^{*\mathrm{m}}(\infty) - n_{ij}^{*\mathrm{m}}(0)}\right] = \frac{y_{ij}^{**} - y_{ij}^*(t)}{y_{ij}^{**} - y_{ij}^{*\infty}} \qquad (8)$$

$$\frac{dn_{ij}^{*\mathrm{m}}}{dt} = -(V\rho)\frac{dy_{ij}^*(t)}{dt} \qquad (9)$$

Relationships analogous to Eqs. (8) and (9) can also be derived using the bulk isotope mole fractions of component i.

Equation (7) shows that the IET technique can be used to estimate the equilibrium GSE of component i (pure gas or mixture) at any chosen values of P, T and y_i by measuring the gas phase mole fractions of the jth trace isotope of component i during the experiment. The key assumptions in deriving Eq. (7) are that the isotherms for adsorption of pure bulk and trace isotopes of component i are identical, and that the selectivities of adsorption between the trace jth isotopes and the bulk isotopes of component i are unity in presence or absence of other components (Rynders et al., 1997).

Equations (8) and (9) show that the kinetics of adsorption of the trace jth isotope of component i at any given P, T and y_i can be evaluated by the IET experiment. A key characteristic of this kinetic process is that (Rynders et al., 1997):

$$\frac{n_{ij}^{*\mathrm{m}}(\mathrm{e})}{y_{ij}^*(t)} = \frac{n_i^{*\mathrm{m}}(\mathrm{e})}{y_i^*(t)} = \frac{n_i^{\mathrm{m}}}{y_i}. \qquad (10)$$

where the variables defined by (e) represents the GSE of the isotopes of component i in equilibrium with the bulk gas phase at P, T and $y_{ij}^*(t)$ or $y_i^*(t)$.

Equations (8)–(10) can be combined with specific mass transfer models for the isotope exchange process in order to obtain analytical expressions for $f_{ij}^*(t)$ in terms of mass transfer coefficients or diffusivities of the isotopes of component i. The linear driving force (LDF) model yields (Rynders et al., 1997):

$$f_{ij}^*(t) = 1 - \exp[(k_{ij}^* a_{ij}^*)t] \tag{11}$$

$$a_{ij}^* = \left[\frac{y_{ij}^{**} - y_{ij}^{*0}}{y_{ij}^{*\infty} - y_{ij}^{*0}}\right] \tag{12}$$

The chemical potential driving force (CPDF) model, which reduces to the conventional Fickian Diffusion model for the IET experiment because of the constraint provided in Eq. (10), yields (Rynders et al., 1997):

$$f_{ij}^*(t) = 1 - \sum_{i=1}^{\infty} \frac{6\alpha(1+\alpha)e^{-\left[D_{ij}^* q_n^2 t/a^2\right]}}{9 + 9\alpha + q_n^2\alpha^2} \tag{13}$$

$$\tan q_n = \frac{3q_n}{3 + \alpha q_n^2}; \quad \alpha = \left[\frac{y_{ij}^{*\infty} - y_{ij}^{*0}}{y_{ij}^{**} - y_{ij}^{*\infty}}\right] \tag{14}$$

Equation (13) applies for isothermal ad(de)sorption on spherical particles of radius a (Crank, 1956).

The mass transfer coefficient (k_{ij}^* in Eq. (11)) and diffusivity (D_{ij}^* in Eq. (13)) for the trace jth isotope of component i, are for self-diffusion under constant P, T, y_i (Kärger and Ruthven, 1992), which can be estimated from the data measured by IET using Eqs. (11)–(14). Furthermore, the simplest way to satisfy the constraint given by Eq. (4) is to assume that the mass transfer coefficients and self-diffusivities of all isotope species (trace and bulk) of component i at any given set of P, T and y_i are equal.

$$k_{ij}^* = k_i^*; \quad D_{ij}^* = D_i^* \tag{15}$$

where k_i^* and D_i^* are the mass transfer coefficient and self diffusivity of bulk isotope of component i at P, T and y_i.

Experimental Apparatus and System

We used a closed loop gas recirculating adsorption system to carry out the IET experiments. Figure 1 is a schematic drawing of the apparatus. The main loop

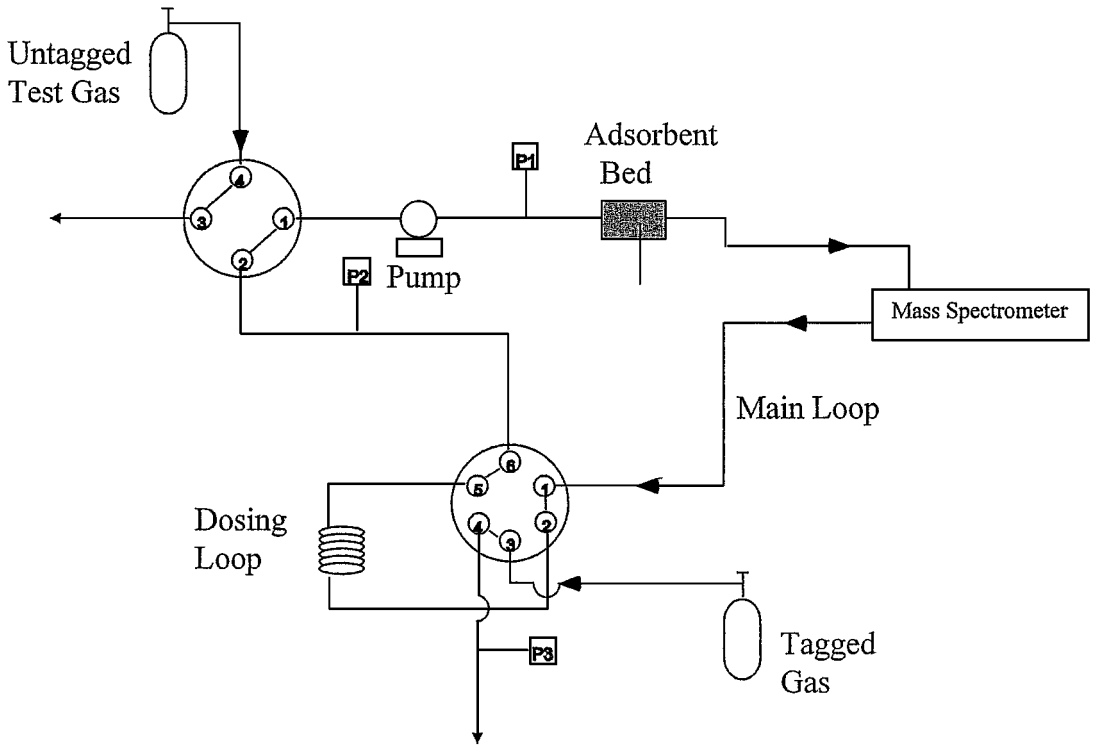

Figure 1. Schematic diagram of IET experimental set up.

Table 1. Physical properties of CH_4 and N_2.

Gas	Kinetic diameter (Å)	Liquid molar volume[a] (cm^3/mol)	Polarizability ($\times 10^{-25}$ cm^3)	Permanent moments: Dipole ($\times 10^{-18}$ esu)	Permanent moments: Quadrupole ($\times 10^{-26}$ esu cm^2)
CH_4	3.80	37.7	26.0	0	0
N_2	3.64	31.6	17.6	0	1.52

[a]At normal boiling point.

(Helium void volume $= V_m$) consists of a packed adsorption chamber, a gas circulating bellows pump, two multiport valves and three pressure transducers (P_1, P_2, P_3). A quadrupole mass spectrometer is used to continuously monitor the gas phase isotope concentrations in the loop by withdrawing a very small quantity of gas (0.33 scc/h) from the system. A dosing loop (Helium void volume $= V_d$) is attached to one of the multiport valves. The entire apparatus is placed within a constant temperature airbath. The adsorbent is first saturated with a gas phase at P, T and y_i (y_{ij}^{*0}). The dosing loop is filled with a gas at P, T and y_i (y_{ij}^{*d}). The dosing loop is then connected with the main loop (total helium volume of the system $V = V_m + V_d$) at the start of the experiment ($t = 0$) and y_{ij}^{*} is monitored as a function of time. A more detailed description of the experimental method is given elsewhere (Rynders et al., 1997). About 30 s were required to mix the dosed and main loop gases. The variable y_{ij}^{**} can be calculated by:

$$y_{ij}^{**} = \left[\frac{V_m y_{ij}^{*0} + V_d y_{ij}^{*d}}{V} \right] \tag{16}$$

The above-described experimental procedure and data analysis method was previously used to measure the pure gas and binary gas equilibria and kinetics for adsorption of N_2 and O_2 on a commercial (Takeda, Japan) sample of carbon moleculer sieve (Rynders et al., 1997). It was found that a mass transfer resistance at the pore-mouth controlled the transport (activated diffusion) of N_2 and O_2 into the nanoporous carbon. The LDF model (Eqs. (11) and (12)) described the transport for both gases. The larger N_2 molecules (diameter = 3.64 Å) diffused slower than the O_2 molecules (diameter = 3.46 Å) creating a kinetic selectively (transient) of adsorption for O_2 over N_2. There was no thermodynamic selectivity of adsorption for these gases on the carbon.

The purpose of this work is to study the pure gas and binary gas equilibria and kinetics for adsorption of CH_4 and N_2 on a commercial (UOP, USA) sample of 4A zeolite (beads: $a = 1.0$ mm) by using the IET method. The adsorbent was regenerated by heating at 400°C under vacuum for 12 h before the adsorption measurements.

Table 1 summarizes the key physical properties of CH_4 and N_2. The molecular diameter of CH_4 (3.8 Å) is larger than that of N_2 (3.64 Å) and they both have sizes comparable to the pore apertures (4.2 Å) of 4A zeolite cavities (Breck, 1984). The N_2 has a small permanent quadrupole moment while CH_4 is nonpolar. However, the polarizability of CH_4 is somewhat larger than that of N_2 (Stogryn and Stogryn, 1966).

The CH_4-N_2-4A zeolite system was previously studied (pure and binary gas adsorption equilibria and kinetics) by Habgood (1958) using conventional volumetric adsorption (pure gas) and total desorption (binary gas) techniques. It was found that the zeolite selectively (thermodynamic) adsorbed CH_4 over N_2. However, the smaller N_2 molecules diffused faster than the larger CH_4 molecules into the zeolite pores during the earlier part of the binary gas uptake process. This initially created a transient N_2 rich adsorbed phase, but a part of the adsorbed N_2 was then displaced by CH_4 to ultimately produce a CH_4 selective adsorbed phase at equilibrium. The larger polarizability of CH_4 was responsible for its thermodynamic selectivity of adsorption over N_2 despite the fact that the zeolite was a highly polar adsorbent and the N_2 had a weak permanent quadrupole.

The experimental methods used by Habgood (1958), however, were very tedious and time consuming. Also they did not warrant isothermal uptake processes. They also did not provide any systematic control over the conditions of measurement (P, T and y_i) of adsorption equilibria and kinetics. The present experimental method alleviates these problems and simplifies model interpretation of the adsorption kinetic data.

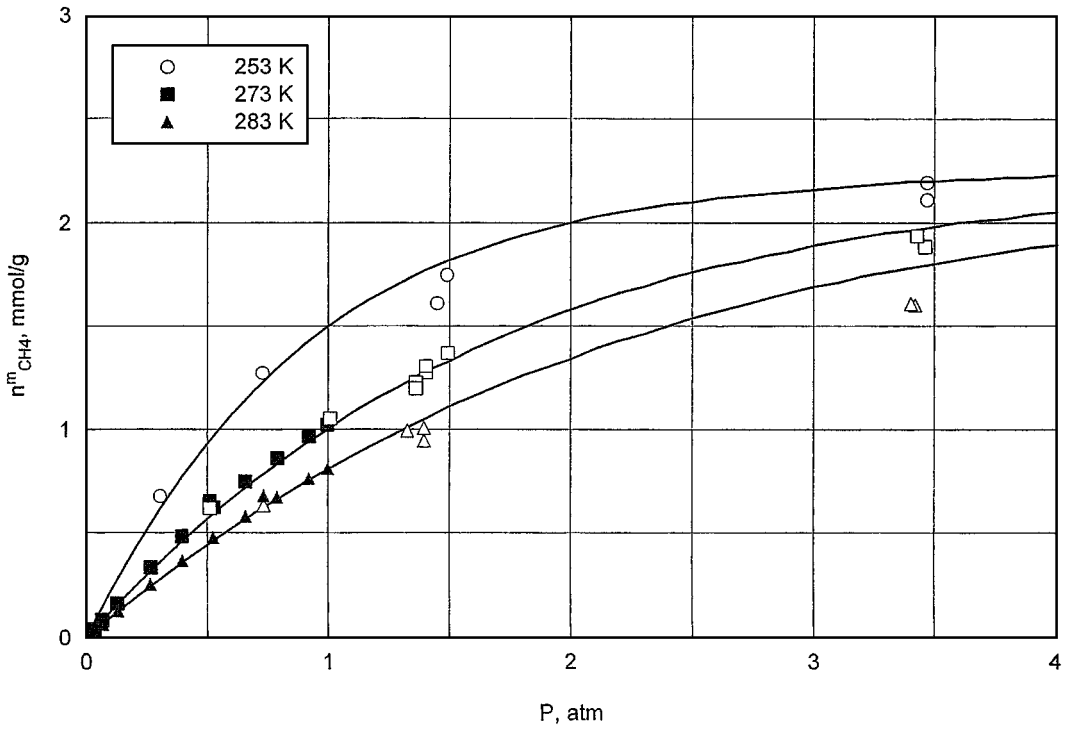

Figure 2. Adsorption isotherms for pure CH_4 on 4A zeolite at 253, 273 and 283 K.

Experimental Results and Discussions

Pure Gas Adsorption Equilibria

The pure gas adsorption isotherms of CH_4 (component 1) and N_2 (component 2) were measured in the pressure range of 0–4 atm on the 4A zeolite sample using IET at 253, 273 and 283 K. Figures 2 and 3 (open symbols) show the adsorption isotherms for CH_4 and N_2, respectively. The GSE are plotted against equilibrium gas phase pressures at constant temperatures. The closed symbols in these figures show the pure gas adsorption isotherms measured independently by using a volumetric adsorption technique described elsewhere (Golden and Sircar, 1994). The figures show that the adsorption isotherms measured by these two methods agree with each other extremely well. The adsorption isotherms for both gases are Type I by the Brunauer classification which is the characteristic of gas adsorption on a microporous solid at low to moderate pressures.

The well known pure gas Langmuir adsorption model could not adequately describe the adsorption isotherms over the ranges of the data using the same saturation adsorption capacities for both gases (required for application of mixed gas Langmuir adsorption model). However, the multi-site Langmuir (MSL) adsorption model (Nitta et al., 1984) could be used to describe the data of Figs. 2 and 3 fairly well as shown by the solid lines in these figures. The average deviations between the calculated and experimental isotherms for the pure gases were within ±5.0% over the entire range of the data. The MSL model is an extension of the Langmuir adsorption model to account for different sizes of adsorbates. For adsorption of a pure gas i, the MSL model gives:

$$K_i P = \frac{\theta_i^0}{\left[1-\theta_i^0\right]^{a_i}} \tag{17}$$

where $\theta_i^0 (n_i^m/m_i)$ is the fractional surface coverage for pure gas i, m_i is the saturation capacity of adsorption for pure gas i, a_i is the number of adsorption sites occupied by each molecule of pure gas i, K_i is the Henry's Law constant in the θ_i^0-P domain ($K_i = (\frac{\delta\theta_i^0}{\delta P})_T$ at the limit of $P \to 0$). Equation (17) reduces to the Langmuir adsorption model when $a_i = 1$. m_i and a_i are temperature independent parameters and a constraint for

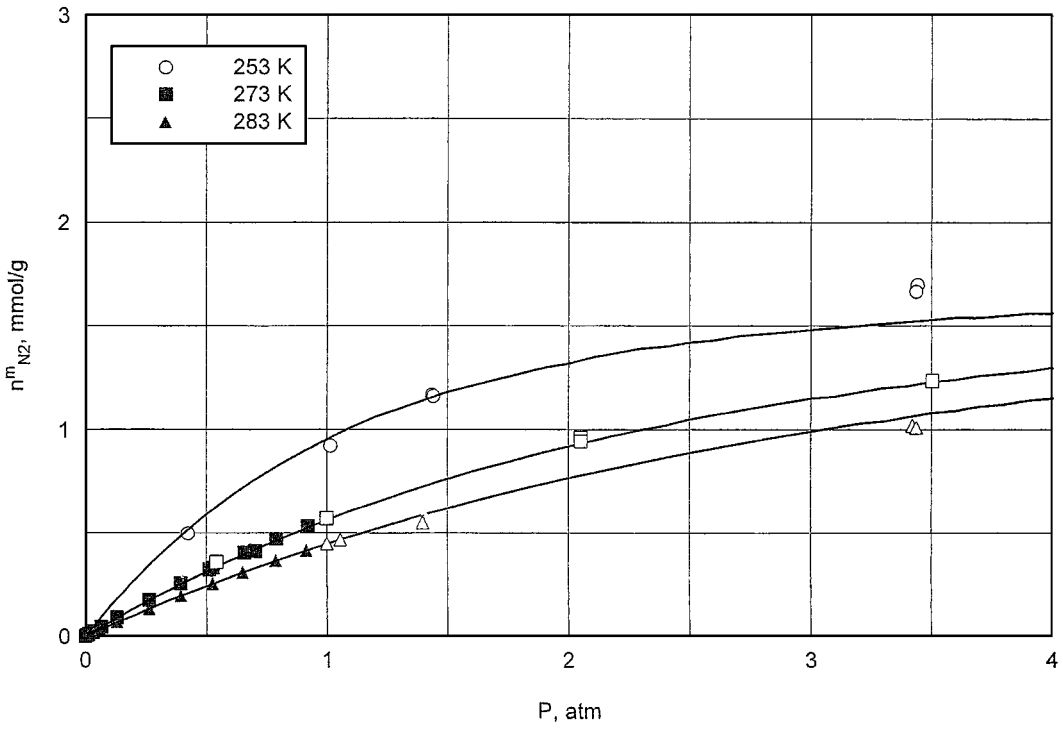

Figure 3. Adsorption isotherms for pure N_2 on 4A zeolite at 253, 273 and 283 K.

the MSL model is:

$$m_i a_i = \text{constant} \tag{18}$$

The MSL model is derived for an energetically homogeneous adsorbent where the isosteric heat of adsorption of pure gas $i\,(q_i^0)$ is independent of θ_i^0:

$$q_i^0 = +RT^2\left[\frac{\delta \ln P}{\delta T}\right]_{\theta_i^0} = -RT^2\left[\frac{d\ln K_i}{dT}\right] \tag{19}$$

Table 2 summarizes the best fit MSL model parameters for adsorption of CH_4 and N_2 on the 4A zeolite using the constraint of Eq. (18). The saturation capacity for CH_4 adsorption is 35.3% larger than that for N_2 while the isosteric heat of adsorption of pure CH_4 (4.2 kcal/mol) is about 13% lower than that for N_2 (4.7 kcal/mol). The Henry's Law constants for CH_4 adsorption isotherms at any temperature are larger than the corresponding Henry's Law constants for N_2.

The ability of the MSL model to fit the pure gas CH_4 and N_2 adsorption isotherms on 4A zeolite indicate that the zeolite is energetically homogeneous (constant q_i^0) for both gases in the range of the data. This is also verified by independently calculating q_i^0 from the isotherms using Eq. (19).

Table 2. Pure gas multisite langmuir model parameters for 4A zeolite.

Gas	T(K)	K_i (mol/kg/atm)	a_i (sites/molecule)	m_i (mol/kg)	q_i^0 (kcal/mol)
CH_4	253	2.30	0.4091	2.30	4.2 ± 0.1
	273	1.27			
	283	0.96			
N_2	253	1.47	0.5535	1.70	4.7 ± 0.3
	273	0.69			
	283	0.52			

The pure gas CH_4 and N_2 adsorption isotherms on 4A zeolite crystals ($a = 0.25\,\mu m$, UCC, USA) reported by Habgood (1958), were measured at 193 and 273 K in the pressure ranges of 0–3 atm. The adsorbent was regenerated by heating at 400°C under vacuum for 1–3 h. The data was described by the Langmuir model. However, the Langmuirian saturation capacity for CH_4 was generally higher than that for N_2 and they were functions of temperature. This would prevent the use of mixed gas Langmuir model for testing binary adsorption data. The isosteric heat of adsorption of CH_4 at the Henry's law limit (5.4 kcal/mol) was slightly higher than that for N_2 (5.1 kcal/mol). The isosteric heats for both gases decreased slightly with increasing surface coverage (inconsistent with Langmuir model).

Binary Gas Adsorption Equilibria

The IET was used to measure the binary gas adsorption isotherms for CH_4 (1) + N_2 (2) mixtures using different total gas pressures (P) and gas compositions (y_i) at three different system temperatures (T). Table 3 summarizes the results. Table 3 also gives the experimental selectivity of adsorption of CH_4 over N_2 from their binary mixtures ($S_{12}^{m} = n_1^{m} y_2 / n_2^{m} y_1$) at the corresponding values of P, T and y_i.

It may be seen from Table 3 that CH_4 is selectively adsorbed over N_2 ($S_{12}^{m} > 1$) but S_{12}^{m} is a weak function of P, T and y_i. The weak temperature dependence of S_{12}^{m} is caused by the nearly equal isosteric heats of adsorption of CH_4 and N_2 on the zeolite. Table 3 also shows that S_{12}^{m} generally decreases with decreasing P (decreasing total GSE, $n^{m} = \sum_i n_i^{m}$) at constant values of T and y_i. This is a very unusual behavior. S_{12}^{m} is independent of P and y_i at constant T for Langmuirian adsorbates and S_{12}^{m} typically decreases with increasing P at constant T and y_i (Sircar, 1996b) for most other systems. The observed behavior, on the other hand, is predicted by the MSL model for the special case where $S_{12}^{m} > 1$ and $a_2 > a_1$ (Sircar, 1995). The multicomponent MSL model (Nitta et al., 1984) yields:

$$K_i P y_i = \frac{\theta_i}{\left[1 - \sum_i \theta_i\right]^{a_i}} \quad i = 1, 2, \ldots \tag{20}$$

where $\theta_i (= n_i^{m}/m_i)$ is the fractional coverage of the ith component of a gas mixture at P, T and y_i. The variables K_i, m_i and a_i are the pure gas MSL model parameters. It can be analytically shown from Eq. (20)

Table 3. Binary adsorption isotherms for $CH_4(1) + N_2(2)$ mixtures on 4A zeolite.

			n_1^{m} (mol/kg)			n_2^{m} (mol/kg)				
T (K)	P (atm)	V_1	Experiment	MSL model	Error (%)	Experiment	MSL model	Error (%)	S_{12}^{m}	θ
253	3.715	0.217	0.776	0.666	−14.2	1.244	1.070	−13.9	2.25	0.918
	1.014	0.241	0.472	0.400	−15.3	0.708	0.700	−1.1	2.10	0.582
	0.513	0.226	0.263	0.222	−15.6	0.460	0.455	−1.1	1.96	0.364
	3.269	0.482	1.487	1.287	−13.5	0.663	0.613	−7.5	2.41	0.924
	2.056	0.495	1.259	1.135	−9.9	0.550	0.573	4.2	2.34	0.838
	0.691	0.504	0.705	0.614	−12.9	0.346	0.357	3.2	2.01	0.510
273	2.862	0.238	0.577	0.534	−6.9	0.762	0.783	6.3	2.42	0.693
	1.008	0.247	0.288	0.264	−8.3	0.431	0.410	−2.8	2.04	0.356
	0.523	0.249	0.165	0.151	−8.5	0.254	0.239	−5.9	1.56	0.206
	3.425	0.496	1.234	1.138	−7.8	0.475	0.502	5.7	2.64	0.790
	2.081	0.503	0.950	0.887	−6.6	0.395	0.413	4.6	2.38	0.628
	0.703	0.538	0.358	0.418	16.8	0.161	0.185	14.9	2.01	0.291
283	3.512	0.520	1.227	1.050	−14.4	0.447	0.438	−2.0	2.53	0.714
	2.128	0.527	0.899	0.783	−12.9	0.345	0.340	1.5	2.33	0.541
	1.499	0.532	0.705	0.611	−13.3	0.282	0.269	−4.6	2.20	0.424
	0.676	0.508	0.330	0.300	−9.1	0.143	0.151	5.6	2.24	0.218
				Average: ±11.0%			Average: ±5.3%			

that S_{12}^{m} decreases with decreasing total surface coverage ($\theta = \sum_i \theta_i$) when $a_2 > a_1$. The θ values for each binary experimental data points are given in Table 3.

Table 3 also shows the calculated values of GSE for binary CH_4 and N_2 adsorption (n_i^{mc}) on the zeolite using Eq. (20) and the pure gas MSL parameters of Table 2. It may be seen that the average error $[\{(n_i^{mc} - n_i^{m})/n_i^{mc}\} \times 100]$ in calculating the mixture GSE for CH_4 and N_2 from the corresponding pure component adsorption isotherms by the MSL model are less than, respectively, 11.0 and 5.6%. However, the methane capacity from the mixture was generally underpredicted by the MSL model. The model, on the other hand, describes the curious effects of adsorbate size differences on the mixture adsorption.

The 4A zeolite selectively adsorbs CH_4 over N_2 even though the isosteric heat of adsorption of CH_4 is somewhat lower than that for N_2. This is because the Henry's Law selectivity (S_{12}^{mo}) of CH_4 over N_2 ($S_{12}^{mo} = K_1 m_1 / K_2 m_2$) is larger than unity.

Pure Gas Self-Diffusion Coefficients

A typical example of pure CH_4 uptake on 4A zeolite measured by IET is shown in Fig. 4. The experiment was carried out by initially saturating the zeolite with pure CH_4 at a pressure of 1.5 atm and at a temperature of 253 K. The corresponding GSE for CH_4 was 1.70 mol/kg. The uptake was measured by monitoring the concentration of trace C^{14} isotope. The diffusion of CH_4 into the zeolite was relatively slow. It took about 40 min to reach a new isotope equilibrium state.

The dashed line of Fig. 4 is the best fit of the experimental data by the Fickian Diffusion or CPDF model. The solid lines in Fig. 4 are uptake curves calculated by the LDF model using different values of mass transfer coefficients. It is obvious from Fig. 4 that the self-diffusion of CH_4 into the 4A zeolite is best described by the Fickian Diffusion model. The value of the diffusion coefficient (D/a^2) is given in the figure.

Figure 5 is a typical example of pure N_2 uptake on the zeolite measured by IET. It was measured by monitoring the concentration of N^{15} isotope. The zeolite, in this case was initially saturated with pure N_2 at a pressure of 1.4 atm and at a temperature of 253 K. The corresponding GSE for N_2 was 1.17 mol/kg. The dashed line in Fig. 5 is the best fit of the uptake data by the Fickian diffusion or CPDF model while the solid lines represent a family of uptake curves according to the LDF model. Thus, it is again clear that the

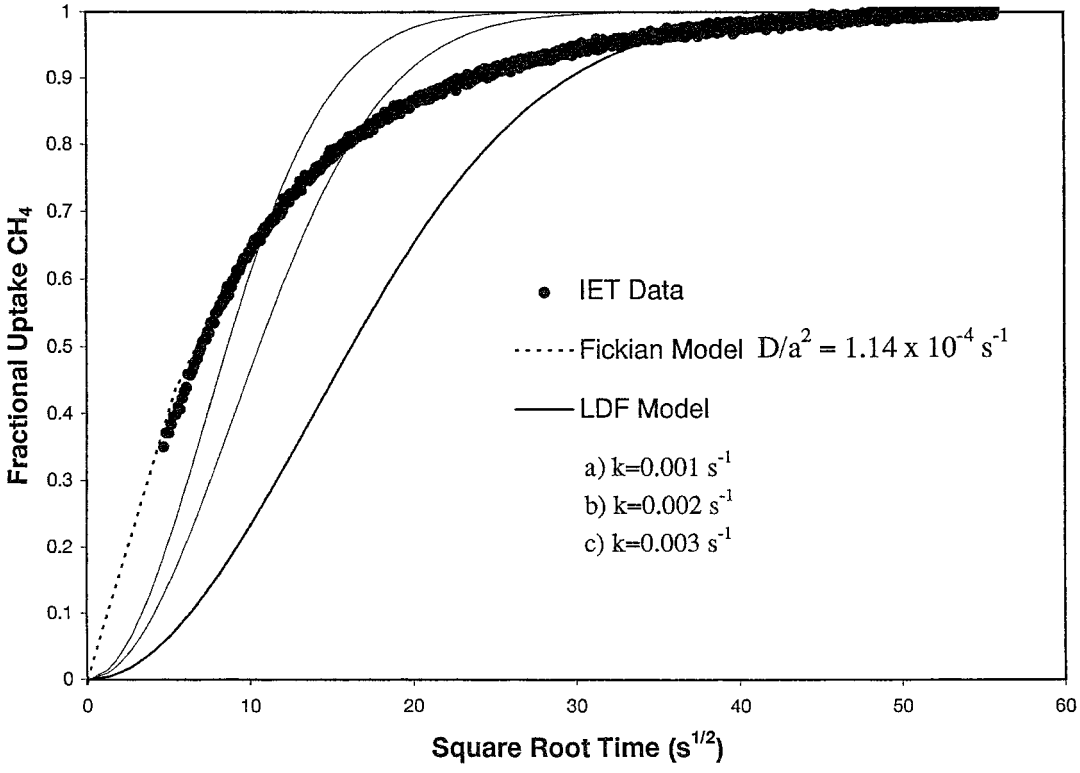

Figure 4. Fractional uptake of pure CH_4 on 4A zeolite at 253 K and 1.5 atm.

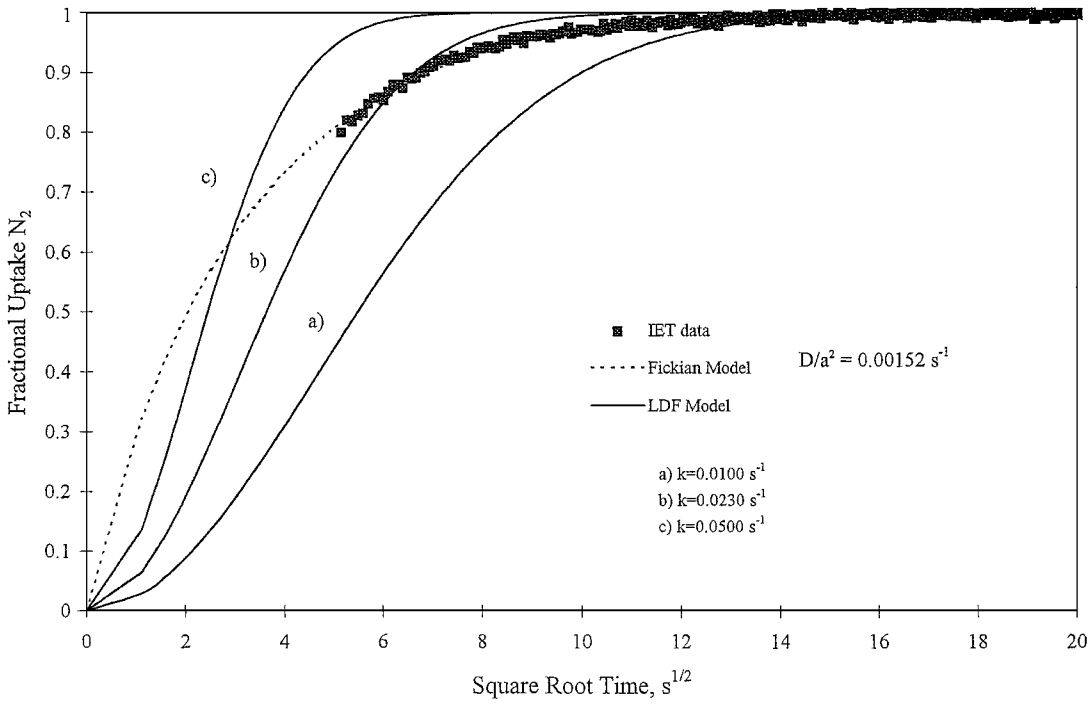

Figure 5. Fractional uptake of pure N_2 on 4A zeolite at 253 K and 1.4 atm.

self-diffusion of N_2 into the zeolite is also described by the Fickian Diffusion model. The value of the diffusion coefficient (D/a^2) is given in the figure. Isotopic equilibration on 4A zeolite was reached much faster by N_2 ($\sim$3.75 min) than CH_4.

A period of about 30 s was required to mix the gases from the dosing loop and the main loop after initial contact ($t = 0$). The gas phase isotope concentrations ($y^*_{ij}(t)$) could not be reliably measured during this period. That is the reason for the absence of uptake data in the early time regions of Figs. 4, 5 and 8. The mixing time of the apparatus must be reduced when the IET method is used to study very fast kinetic systems.

The IET was used to measure the self-diffusivities of pure CH_4 and N_2 on the zeolite as functions of fractional surface coverage (θ^0_i) at three different temperatures. The saturation capacities of pure gas MSL model were used to calculate θ^0_i. Figures 6 and 7 show the results for CH_4 and N_2 respectively. The CH_4 diffusivities remain practically constant over a fairly large range of surface coverages ($0 \le \theta^0_i < 0.5$) and then they increase as θ^0_i increases. This behavior is observed at all temperatures of the experiment. The N_2 diffusivities, on the other hand, remain constant in the entire range of the data at all temperatures. It should be noted here that the present study contains more extensive data for N_2 in the low coverage range than previously published (Rynders et al., 1997). These additional data indicate that the pure N_2 self-diffusivity remains fairly constant over a large range of coverage and does not decrease with increasing coverage as previously believed.

Table 4 reports the self-diffusivities (D_i/a^2) of pure CH_4 and N_2 at the limit of zero surface coverage ($\theta^0_i \to 0$) obtained by extrapolation of the data reported in Figs. 6 and 7, respectively. The limiting self-diffusivity of CH_4 is an order of magnitude smaller than that of N_2. The diffusion process is activated:

$$D^0_i = D^{00}_i \exp\left[-E^0_i/RT\right] \tag{21}$$

Table 4. Limiting self-diffusivities of CH_4 and N_2 on 4A zeolite.

	D^0_i/a^2 ($\times 10^4\ s^{-1}$)		E^0_i (kcal/mol)	
T (K)	CH_4	N_2	CH_4	N_2
253	0.95	14.0	6.5 ± 0.3	5.5 ± 0.3
273	2.5	30.0		
283	3.8	44.0		

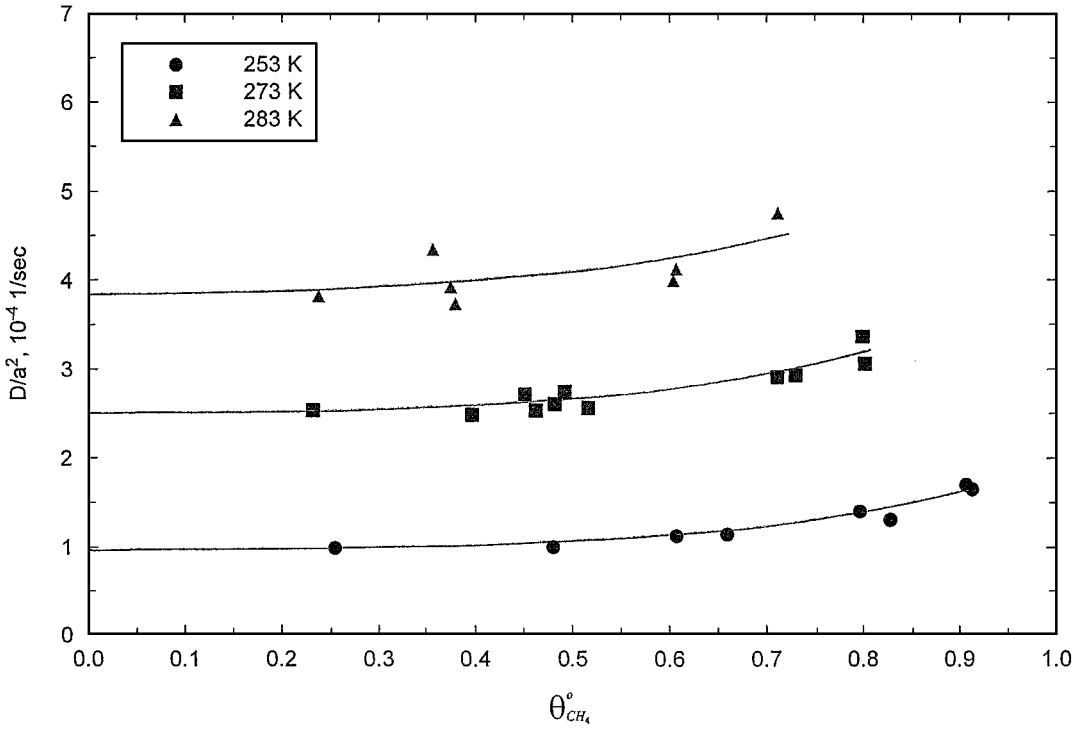

Figure 6. Self-diffusivities of pure CH_4 on 4A zeolite as functions of surface coverages at 253, 273 and 283 K.

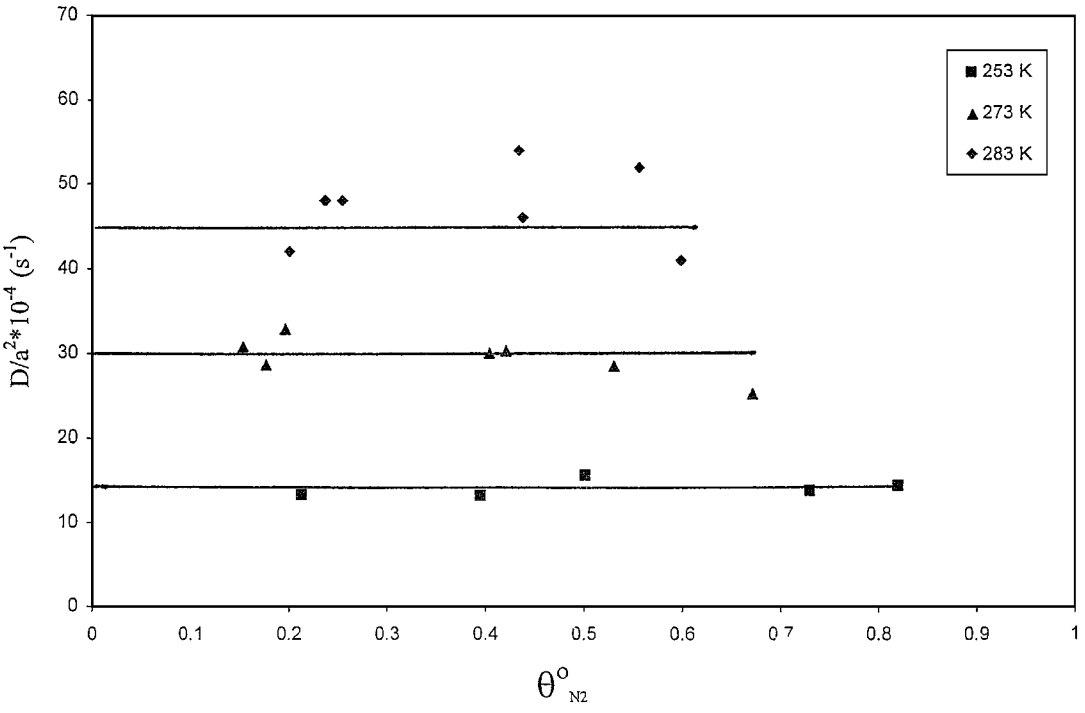

Figure 7. Self-diffusivities of pure N_2 on 4A zeolite as functions of surface coverages at 253, 273 and 283 K.

where E_i^0 is the activation energy for self-diffusion of pure gas i at the limit of $\theta_i^0 \to 0$. R is the gas constant and D_i^{00} is a constant. Table 4 shows that E_i^0 for CH_4 is somewhat larger than that for N_2.

Binary Gas Self-Diffusion Coefficients

The IET was used to measure binary CH_4-N_2 self-diffusivities on 4A zeolite at three different temperatures using different absorbate loadings. Figure 8 is a typical example of the binary uptake process. The conditions for the equilibrium state of this experiment were, $P = 0.691$ atm, $T = 253$ K, $y_i = 0.50$. The corresponding equilibrium GSE for CH_4 and N_2 were respectively, 0.723 and 0.354 mol/kg. The isotopic concentrations of C^{13} and N^{15} were monitored in these experiments.

It may be seen from Fig. 8 that N_2 reaches the new isotopic equilibrium state much faster than CH_4 as expected. The solid lines in Fig. 8 show the best fit of the uptake curves by the Fickian Diffusion or CPDF model. The corresponding diffusivities of the components are given in the figure. The Fickian Diffusion model was found to describe all binary CH_4-N_2 uptake data very well.

Table 5 summarizes the results of the binary diffusion tests. They were measured at 253, 273 and 283 K using different total gas pressures ($P = 0.7$–3.5 atm). The gas phase mole fractions of CH_4 were varied in the range of 0.2–0.5. The corresponding fractional coverages (θ_i) of CH_4 and N_2 at appropriate values of P, T and y_i were calculated ($\theta_i = n_i^*/m_i$) by using MSL model saturation capacities for the adsorbates.

It may be seen from Table 5 that the self-diffusivities of CH_4 and N_2 from their mixtures do not significantly vary as functions of P for a given T and y_i even though θ_i vary significantly. Another interesting characteristic of the mixed gas diffusivities of the present system is demonstrated by the last column in Table 5. It gives the ratio (ψ) of the component self-diffusivities of the mixture to the pure gas self-diffusivities of components at the same values of $\theta_i^0 (= \theta_i)$ and T. The parameter ψ for both CH_4 and N_2 is nearly unity. This suggests that the self-diffusivities of CH_4 and N_2 are not affected by the presence of each other under the test conditions of Table 5. The external gas film transport resistances for the jth isotope of component i were estimated to be less than 3.0% of the overall transport resistances (Rynders et al., 1997) under the conditions of IET experiments reported in this work.

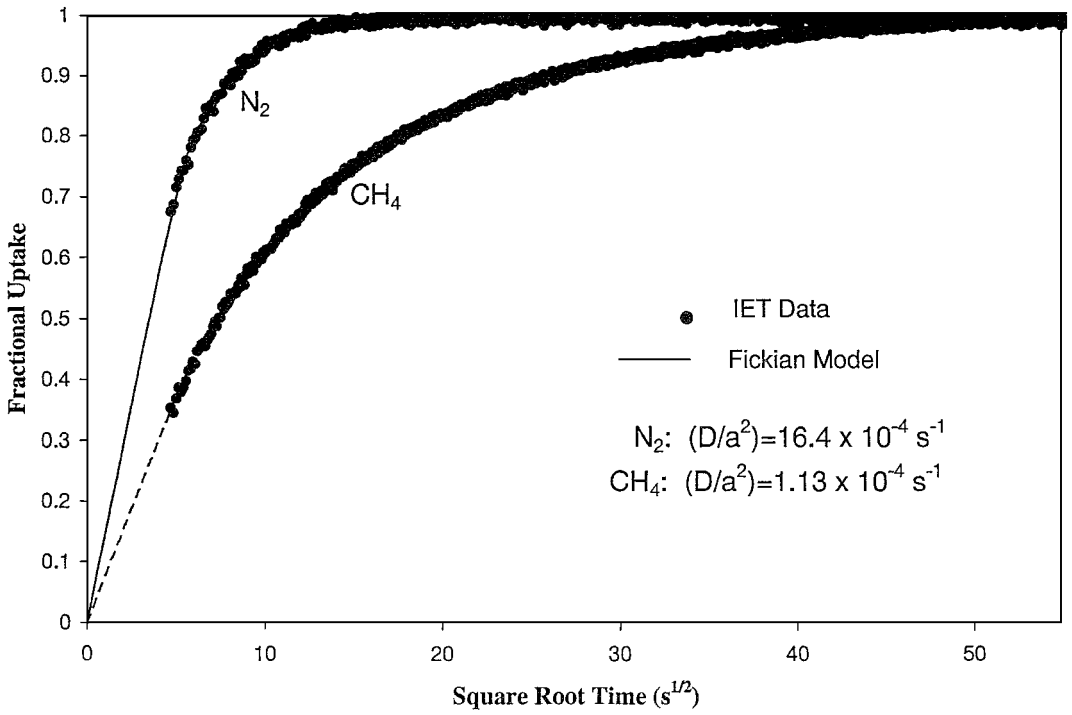

Figure 8. Fractional uptakes of CH_4 and N_2 from their equimolar binary mixtures on 4A zeolite at 253 K and 0.69 atm.

Table 5. Self-diffusivities of CH_4 and N_2 from their binary mixtures on 4A zeolite.

					(D_i/a^2) $(\times 10^4\ s^{-1})$		ψ	
P (atm)	T (K)	${}^{y}CH_4$	${}^{\theta}CH_4$	${}^{\theta}N_2$	CH_4	N_2	CH_4	N_2
3.715	253	0.217	0.289	0.534	0.971	13.6	0.97	0.971
1.014	253	0.241	0.175	0.304	0.84	14.0	0.84	0.999
0.512	253	0.226	0.097	0.197	0.88	14.6	0.93	1.041
3.269	253	0.482	0.551	0.284	1.13	16.5	1.03	1.177
2.056	253	0.495	0.466	0.236	1.02	15.2	1.02	1.087
0.69	253	0.504	0.261	0.148	0.97	16.2	0.97	1.157
2.861	273	0.238	0.214	0.327	2.61	30.0	1.05	1.000
1.008	273	0.247	0.107	0.185	2.41	30.3	0.96	1.010
0.524	273	0.249	0.049	0.109	2.34	30.2	1.00	1.007
3.425	273	0.496	0.457	0.204	2.58	32.9	1.00	1.097
2.080	273	0.503	0.352	0.170	2.53	35.2	1.00	1.172
0.712	273	0.538	0.183	0.091	2.37	28.6	0.95	0.953
3.511	283	0.520	0.454	0.192	3.87	41.3	0.97	0.938
2.127	283	0.527	0.333	0.148	3.82	46.6	0.97	1.059
1.498	283	0.532	0.261	0.121	3.62	43.9	0.93	0.997
0.676	283	0.508	0.122	0.061	3.78	42.6	0.98	0.967

Habgood (1958) measured transport diffusivities (under non-equilibrium condition) of CH_4 and N_2 as pure gases as well as binary mixtures on 4A zeolite crystals at several temperatures. The experimental uptake could be described by the conventional isothermal Fickian Diffusion model (Crank, 1956) which gives a linear plot of fractional uptake against $\sqrt{t}$ in the low time region. It was found that (a) the pure CH_4 diffusivity is an order of magnitude slower than that for pure N_2, and (b) the pure gas transport diffusivity increased with increasing surface coverage (θ_i^0) approximately following the Darken correction for adsorption isotherm non-linearity (Kärger and Ruthven, 1992). The N_2 diffused into the zeolite crystal much faster than CH_4 from their binary mixtures creating a transient N_2 enriched adsorbed phase. It also caused the fractional uptake-time plot of N_2 to go through a maximum while the corresponding plot for CH_4 monotonically increased. Approximate calculation of mixed gas diffusivities indicated that (a) the CH_4 diffusivity in presence of N_2 was similar to that of pure CH_4 diffusivity and (b) the N_2 diffusivity in presence of CH_4 was significantly increased compared to the pure gas diffusivity.

This study shows that the self diffusivities of both CH_4 and N_2 from their mixtures are not affected by the presence of each other, which is not the case for transport diffusivity of N_2.

Summary

The isotope exchange technique (IET) is demonstrated to be a powerful tool for simultaneous measurement of pure and binary gas adsorption equilibria and kinetics in a single isothermal experiment without disturbing the adsorbed phase. The technique is used to study adsorption of pure CH_4 and N_2 and their binary mixtures on 4A zeolite pellets at different temperatures. The pure gas and binary gas adsorption isotherms can be adequately described by the multi-site Langmuir model. CH_4 is selectively adsorbed over N_2. The selectivity is found to increase with increasing gas pressure at constant temperature and gas phase composition which is an uncommon effect of differences in adsorbate sizes. The self diffusion of CH_4 and N_2 as pure gas or as mixtures into the zeolite cavity can be described by the Fickian Diffusion model. The diffusion is an activated process and the diffusivity of CH_4 is an order of magnitude smaller than that of N_2 even though the difference between their molecular diameters is only 0.20 Å. The diffusivities of CH_4 and N_2 from their mixtures are not affected by the presence of each other.

Nomenclature

a = Radius of adsorbent particle
a_{ij}^* = Function defined by Eq. (12)
a_i = Number of adsorption sites per molecule of pure gas i
D_{ij}^* = Self-diffusivity of trace jth isotope of component i
D_i^* = Self-diffusivity of bulk isotope of component i
D_i^0 = Limiting value of D_i^* at zero surface coverage
D_i^{00} = Constant defined by Eq. (21)
E_i^0 = Activation energy for self-diffusion of pure gas i at zero surface coverage
f_{ij}^* = Fractional uptake of trace jth isotope of component i
J_{ij}^* = Flux of trace jth isotope of component i
J_i^* = Flux of bulk isotope of component i
J_i = Total flux of component i
k_{ij}^* = Mass transfer coefficient for self-diffusion of trace jth isotope of component i
k_i^* = Mass transfer coefficient for self-diffusion of bulk isotope of component i
K_i = Henry's Law constant for component i (θ_i^0-P domain)
m_i = Saturation capacity (GSE) of pure gas i
$n_{ij}^{*\mathrm{m}}$ = Surface excess of trace jth isotope of component i
$n_i^{*\mathrm{m}}$ = Surface excess of bulk isotope of component i
n_i^{m} = Surface excess of component i
n^{m} = Total surface excess of all components
n_i^{mc} = Calculated surface excess of component i
n_i^{a} = Actual specific amount adsorbed of component i
P = Gas phase pressure
q_i^0 = Isosteric heat of pure gas i
q_n = Parameter defined by Eq. (14)
R = Gas Constant
S_{12}^{m} = Measured selectivity of adsorption of component 1 over component 2
S_{12}^{mo} = Henry's Law selectivity at the limit of $P \to 0$
T = System temperature
t = Time
v^{a} = Actual specific volume of adsorbed phase
V_{m} = Specific helium volume of main loop
V_{d} = Specific helium volume of dosage loop
V = Total specific helium volume of IET loop
y_{ij}^* = Mole fraction of trace jth isotope of component i
y_i^* = Mole fraction of bulk isotope of component i
y_i = Total mole fraction of component i

Greek Letters

α = Parameter defined by Eq. (14)
ρ = Gas phase density
θ_i^0 = Fractional surface coverage of pure gas i
θ_i = Fractional surface coverage of gas i from mixture
θ = Total fractional surface coverage of all components

Superscripts

$*_0$ = Initial gas phase saturation conditions on adsorbent
$**$ = Gas phase conditions on adsorbent at start of IET
$*_\infty$ = Gas phase conditions on adsorbent at end of IET

Subscripts

i = Component i
ij = Trace jth isotope of component i

Other scripts

(0) = In equilibrium with conditions at start of IET
(∞) = In equilibrium with conditions at end of IET
(e) = In equilibrium with conditions at time t

Acknowledgment

The authors are grateful to J.M. Shabrach for carrying out some of the IET experiments.

References

Breck, D.W., *Zeolite Molecular Sieves*, R.E. Krieger Publishing, Malabar, Florida, 1984.
Crank, J., *Mathematics of Diffusion*, Oxford University Press, London, 1956.
Gibbs, J.W., *The Collected Works of J.W. Gibbs*, Longmans and Green, New York, 1928.
Golden, T.C. and S. Sircar, "Gas Adsorption on Silicalite," *J. Colloid and Interface Sci.*, **162**, 182 (1994).

Habgood, H.W., "The Kinetics of Molecular Sieve Action, Sorption of Nitrogen-Methane Mixtures By Linde Molecular Sieve 4A," *Can. J. Chem.*, **36**, 1384 (1958).

Kärger, J. and D.M. Ruthven, *Diffusion in Zeolites*, Wiley-Interscience, New York, 1992.

Nitta, T., T. Shigetomi, M. Kuro-oka, and T. Katayama, "An Adsorption Isotherm of Multi-Site Occupancy Model for Homogeneous Surface," *J. Chem. Eng.*, Japan, **17**, 39 (1984).

Rynders, R.M., M.B. Rao, and S. Sircar, "Isotope Exchange Technique for Measurement of Gas Adsorption Equilibria and Kinetics," *AIChE J.*, **43**, 2456 (1997).

Sircar, S., "Excess Properties and Thermodynamics of Multicomponent Gas Adsorption," *J. Chem. Soc. Faraday Trans. I*, **81**, 1527 (1985).

Sircar, S., "Influence of Adsorbate Size and Adsorbent Heterogeneity on IAST," *AIChE J.*, **41**, 1135 (1995).

Sircar, S., "Data Representation for Binary and Multicomponent Gas Adsorption Equilibria," *Adsorption*, **2**, 327 (1996a).

Sircar, S., "Adsorption" *Chapter in the Engineering Handbook*, R.C. Dorf (Ed.), pp. 604–617, CRC Press, Boca Raton, Florida, 1996b.

Stogryn, D.E. and A.P. Stogryn, "Molecular Multiple Moments," *Mol. Phys.*, **11**, 371 (1966).